

Development and Optimization of Chitosan Based Film Forming Gel By 2³ Factorial Design

Prashant Kumar Sharma^{1*}, Rajesh Kumar Sharma²

¹*Research Scholar, Teerthanker Mahaveer College of Pharmacy, Teerthanker Mahaveer University, Delhi road, Moradabad, UP*

ORCID ID: 0000-0002-0196-4253

²*Associate Professor, Teerthanker Mahaveer College of Pharmacy, Teerthanker Mahaveer University, Delhi road, Moradabad, UP*

ORCID ID: 0000-0002-3763-8521

ABSTRACT

Background: This study is focused on developing film-forming systems that combine the ease of application of gels with the protective function of traditional bandages. Conventional dressings often require frequent changes, which can disrupt healing and increase infection risks. Film-forming gels address these limitations by transforming from a topical gel into a flexible, adherent film upon contact with the wound epidermis, creating an optimal healing microenvironment.

Objective: The primary objective was to create a wound dressing that effectively shields injuries from external environmental contaminants while preventing microbial growth and infection. This gel-to-bandage system was specifically designed to maintain an optimal healing environment by protecting the wound from spoilage factors and pathogenic microorganisms. The formulation combines the advantages of easy topical application with the protective durability of conventional dressings, offering enhanced wound management through its unique phase transition properties. Key evaluation parameters included the formulation's ability to form a continuous protective film, its antimicrobial efficacy, and its capacity to maintain a sterile wound environment conducive to healing.

Method: A film-forming gel was developed using chitosan, polyvinyl alcohol (PVA), and polyethylene glycol (PEG) as key components. To optimize the formulation, chitosan concentration, PVA content, and PEG ratio were selected as independent variables, while tensile strength, water vapor absorption capacity, and drying time were analyzed as critical dependent response variables. The developed gel was systematically evaluated for essential physicochemical characteristics, including drying time, viscosity, pH, and water vapor absorption properties, to ensure optimal performance and functionality. The method which is adopted for the optimization of the formulation is 2³ factorial design on the Design expert software.

Discussion: The formulation's superior performance over conventional dressings stems from its quick-drying film formation and moisture control, though future studies should validate its antimicrobial efficacy and in vivo healing potential to confirm clinical applicability. The 2³ factorial design effectively optimized critical parameters for wound care applications.

Results: The optimized formulation demonstrated excellent mechanical and physicochemical characteristics, with a tensile strength of $93 \pm 0.01\%$, indicating robust structural integrity. The rapid drying time of 8 ± 0.14 minutes facilitates quick clinical application, while the optimal viscosity (10294 ± 0.5 maP.s) ensures easy spreadability. The formulation maintained skin-compatible pH (5.8 ± 0.5) and showed superior film-forming ability, forming a continuous, flexible protective layer. These combined properties confirm the formulation's suitability as an effective gel-to-bandage wound dressing system, meeting all critical performance criteria for wound protection and healing.

Conclusion: The optimized chitosan/ PVA/PEG film-forming gel demonstrated excellent mechanical strength ($98.34 \pm 0.01\%$), drying (9 ± 0.14 min), and ideal viscosity (10294 ± 0.5 maP.s), proving its effectiveness as a protective wound dressing that combines easy application with durable barrier properties.

Keywords: Film-forming gel, Optimization, Chitosan, Factorial design & Antimicrobial protection

How to cite this article: Sharma PK, Sharma RK, Development and Optimization of Chitosan Based Film Forming Gel By 2³ Factorial Design. *Int J Drug Deliv Technol.* 2026;16(7s): 495-507; DOI: 10.25258/ijddt.16.7s.54

Source of support: Nil.

Conflict of interest: Nil

Topical film-forming systems have become an important area of research because they offer a simple and patient-

INTRODUCTION

*Author for Correspondence: prashantsharma7615@gmail.com

friendly way to deliver therapeutic agents to the skin. When applied, these formulations spread easily and form a thin, flexible film that can remain on the skin surface for an extended period. This helps improve the contact time of the drug with the affected area and can lead to better clinical outcomes. Chitosan, a naturally derived polymer, is widely used in such formulations due to its safety, biodegradability, and its ability to form clear, strong films. Its antimicrobial and wound-protective properties further increase its suitability for use in topical preparations (Pereira et al., 2018).

Creating a film with consistent quality depends on several formulation and process variables. Small changes in the concentration of polymer, plasticizer, or solvent can greatly affect drying time, mechanical strength, flexibility, and overall performance of the film. (Felton, 2013; Montgomery, 2017) Because of this, a systematic method is needed to understand how each factor influences the final product. Factorial design, a part of the Design of Experiments (DoE) approach, offers a structured way to study several variables at the same time. A 2³ factorial design makes it possible to examine three independent factors at two levels each, along with the interactions that may occur between them (Beg et al., 2019).

The present work focuses on the development and optimization of a chitosan-based film-forming system using a 2³ factorial design. This study aims to identify the factors that significantly influence the quality attributes of the film and to obtain a formulation with desirable physical and functional characteristics. By applying a statistical design, the study provides a clearer understanding of formulation behavior and contributes to the development of an effective chitosan film for topical use (Montgomery, 2017; Beg et al., 2019)..

In the market there are many conventional topical preparations available in the form of gels, ointments, or creams available in the market. As these types of the drug delivery system can't provide the sufficient amount of drug release over the site of action. To overcome all these problems we have designed the film forming gel for the drug delivery which will provide the microenvironment to the site at which the drug has delivered for showing the specific response over the site of action. As a consequence, the wound may become infected and fail to heal, ultimately resulting in mortality (Pereira, et al., 2014). For infection prevention, various wound-healing medications, including antibiotics, can be employed (Rodeheaver and Pettry, 1976). Therefore, by giving topical antibiotics as an adjuvant therapy to

systemic dosage and minimizing serious skin damage, appropriate antibiotic therapy should be started as soon as possible.

2. Material and Methods

The pure drug Caffeic Acid was obtained from Central Drug House (P) Ltd – CDH, New Delhi. The Chitosan, Polyvinyl Alcohol (PVA), Acetic Acid and polyethylene glycol (PEG) were obtained from the chemoxy international limited. All other reagents used were of analytical grade.

3. Compatibility study

The physicochemical compatibility of the drug substances with various polymers and excipients was assessed using Fourier-transform infrared spectroscopy (FTIR) and differential scanning calorimetry (DSC).

3.1. Fourier transform infrared spectroscopy

Fourier-transform infrared spectrophotometer (Shimadzu Spectrum – 400 - IR Spirit-X Series) was used to obtain the infrared spectra of the drug, polymer, and their physical mixtures. The objective was to identify any potential interactions between the drug and polymer components

3.2. Differential scanning calorimetry

Differential scanning calorimetry DSC was performed using TGA: DSC TA Instruments Trios V5.4.0.300. The loading puncture was used to load and seal the drug sample into the DSC pan. The sample underwent scanning within the temperature

4. Formulation of film-forming Gel bandage

To prepare the film-forming solution, begin by dissolving chitosan in a 1-3% acetic acid solution, stirring it continuously for 12 to 24 hours until a clear solution is achieved. Simultaneously, prepare a separate polyvinyl alcohol (PVA) solution by dissolving PVA in distilled water with heat at approximately 90°C and constant stirring, then allowing it to cool to room temperature. Next, the active ingredient, caffeic acid, is solubilized in a small volume of distilled water or ethanol, with the addition of an antioxidant such as ascorbic acid to enhance its stability. The two polymer solutions are then combined, and the stabilized caffeic acid solution is introduced slowly under continuous stirring to ensure a homogeneous mixture. To impart flexibility and reduce brittleness in the final film, a plasticizer like polyethylene glycol is incorporated. Finally, the pH of the entire mixture is carefully adjusted

to a skin-compatible range of 5.5 to 6.5 using dilute sodium hydroxide or hydrochloric acid.

5. Experimental design

Experimental design i.e 2³ factorial Design which was used to optimize the film forming gel formulation. In this experimental design various independent & dependent factor was taken that mention in table 1.

Independent Variable/ Factor	Low (-1)	High (+1)	Unit
Chitosan concentration (X ₁)	1%	3%	w/v (%)
PVA concentration (X ₂)	4%	8%	w/v (%)
PEG (Plasticizer) (X ₃)	1%	2%	w/v (%)
Dependent variable	Unit	Goal	
Drug Release (Y1)	%	Maximize	
Drying Time (Y2)	min	Minimize	
Viscosity (Y3)	MPa	Maximize	

Table 1 List of independent and dependent variables for optimization by 2³ Factorial Design

Formulation Code	A:Chitosan Concentration %	B:PVA Concentration %	C:PEG Concentration %
FFG 1	3	4	1
FFG 2	1	8	1
FFG 3	1	4	2
FFG 4	1	4	1
FFG 5	3	8	1
FFG 6	1	8	2
FFG 7	3	4	2
FFG 8	3	8	2

Table 2 : 2³ Factorial design for the drug-loaded Film forming Gel

As per the experimental design over all 8 formulation are generated and got optimized the selection of independent variables was done based on their ability to affect a formulation. The dependent variables highlighted (Table 1) were chosen as crucial parameters in determining formulation. The above analysis employs 9 runs (Table 2) keeping a center point per block 1 and the equation created by the software is given as follows:

$$Y = \beta_0 + \beta_1A + \beta_2B + \beta_3C + \beta_{12}AB + \beta_{13}AC + \beta_{23}BC + \beta_{11}A^2 + \beta_{22}B^2 + \beta_{33}C^2$$

In the above equation, the response of the dependent variable is indicated by Y; β_0 is the intercept, and β_1 to β_{33} indicates the regression coefficient. The concentration of EC (A), DBS (B), and IPM (C) were chosen as the independent variables to be involved in the study while the dependent variables were Drug Release (Y1), Drying Time (Y2), and Viscosity (Y3). Statistical analysis using analysis of variance (ANOVA) was conducted to interpret the outcome of the results. 3D response graphs were also generated employing the software design (Sharma, et al., 2022).

6.1. Characterization of film forming system

6.1.1. Physical Appearance, pH, and viscosity

Uniformity, integrity, color, and clarity were determined by visual method. The pH measurements were carried out by using a pre-calibrated room digital-type pH meter at temperature by contacting the surface of the gel bandage. The brookfield digital viscometer was employed to determine the viscosity of optimized formulation using specific spindle L-4 (Suresh and Abhishek, 2016).

6.1.2. Percent moisture uptake

To check the water resistance capacity of a film, an approximately 100 μ l sample was evenly sprayed onto the glass plate and was left to dry at a temperature of 25 \pm 2 $^{\circ}$ C. Subsequently, the dried film was weighed and introduced into a water bath (HICON, New Delhi, India) held at a constant temperature of 37 $^{\circ}$ C. After a period of 24 h, the film was taken out, gently wiped with tissue paper, and reweighed and examined (Aggarwal et al., 2022 & Walendziak et al., 2021) using the formula:

$$\% \text{ Moisture Content} = \frac{W_w - W_d}{W_w} \times 100$$

Where,

W_w = Wet weight.

W_d = Dry weight.

6.2.3. Stickiness of Gel bandage

The assessment of outward stickiness was carried out by applying cotton wool to the dry film under very slight pressure (Süntar et al., 2013). The stickiness was assessed as high (densely accumulated), medium (few fibers), or low (no or occasional fibers) based on the amount of fibers that adhere to the film (Lodhi et al., 2016).

6.2.4 Tensile strength and drying time

The mechanical properties of the prepared films were assessed using a tensile testing apparatus in accordance with the ASTM D882-02 standard guidelines. As per these guidelines, films with a thickness of less than 1 mm are suitable for tensile strength determination. The test was conducted using a constant rate-of-grip separation method, which involves maintaining a uniform rate of separation between the grips that hold the ends of the test specimen. Film samples were cut into rectangular strips and subjected to testing at a crosshead speed of 1 mm/min.

The tensile strength (N/mm²) of each sample was calculated using the following equation:

$$\text{Tensile Strength (N/mm}^2\text{)} = \frac{N \text{ break}}{A \text{ sample}}$$

The drying time of the Film forming gel formulation was evaluated using the glass slide method. A measured amount of the formulation was sprayed onto the inner forearm of a volunteer, and a clean glass slide was gently placed over the applied area after 5 minutes. The film was considered dry if no liquid residue was observed on the glass slide upon removal. If any liquid traces remained, the test was repeated, extending the drying duration to 7 minutes to ensure complete film formation (Febriyenti et al., 2010).

6.2.5 Stickiness of film forming gel

The assessment of outward stickiness was carried out by applying cotton wool to the dry film under very slight pressure (Süntar et al., 2013). The stickiness was assessed as high (densely accumulated), medium (few fibers), or low (no or occasional fibers) based on the amount of fibers that adhere to the film (Lodhi et al., 2016).

6.2.6. In-vitro release studies

In-Vitro drug release investigations were carried out utilizing a Franz diffusion cell. The films generated by spraying at a consistent period were sliced into 1 cm² and deposited on a pre-treated cellulose acetate membrane to conduct the in-vitro drug release investigations. The membrane was fixed to the diffusion cell with the drug-discharging surface of the film facing

the receptor compartment (Tas et al., 2003). The receptor compartment was filled with phosphate buffer (PBS) of pH 5.8 at a temperature of 37 ± 0.5 °C and stirred magnetically at a speed of 100 rpm. A sample of the dissolving media (2 ml) was extracted and replaced with a new dissolution medium at each time interval. The percent drug release from the withdrawn samples was determined by Ultra Violet Spectrophotometer (UV). The obtained data was subsequently subjected to fitting against multiple mathematical models, including zero-order, first-order, second-order, Higuchi, and Korsmeyer-Peppas models. Among these models, the formulation exhibiting the highest R² value was determined to be the most suitable model for describing drug release behavior.

7 Results

7.1.1. Fourier transform infrared spectroscopy (FTIR)

The FTIR spectrum of the Caffeic acid–Chitosan complex showed a broad band at $3433\text{--}3237\text{ cm}^{-1}$ due to overlapping O–H and N–H stretching, indicating hydrogen bonding. The peaks at 1647 cm^{-1} (amide I) and 1531 cm^{-1} (amide II) confirm interaction between caffeic acid and chitosan. Bands at 1599 cm^{-1} and $1450\text{--}1374\text{ cm}^{-1}$ correspond to aromatic C=C and O–H vibrations of caffeic acid, while peaks at $1278\text{--}1120\text{ cm}^{-1}$ represent C–O and C–O–C stretching of the chitosan backbone. These observations confirm successful incorporation of caffeic acid into chitosan through hydrogen bonding and possible amide linkage formation.

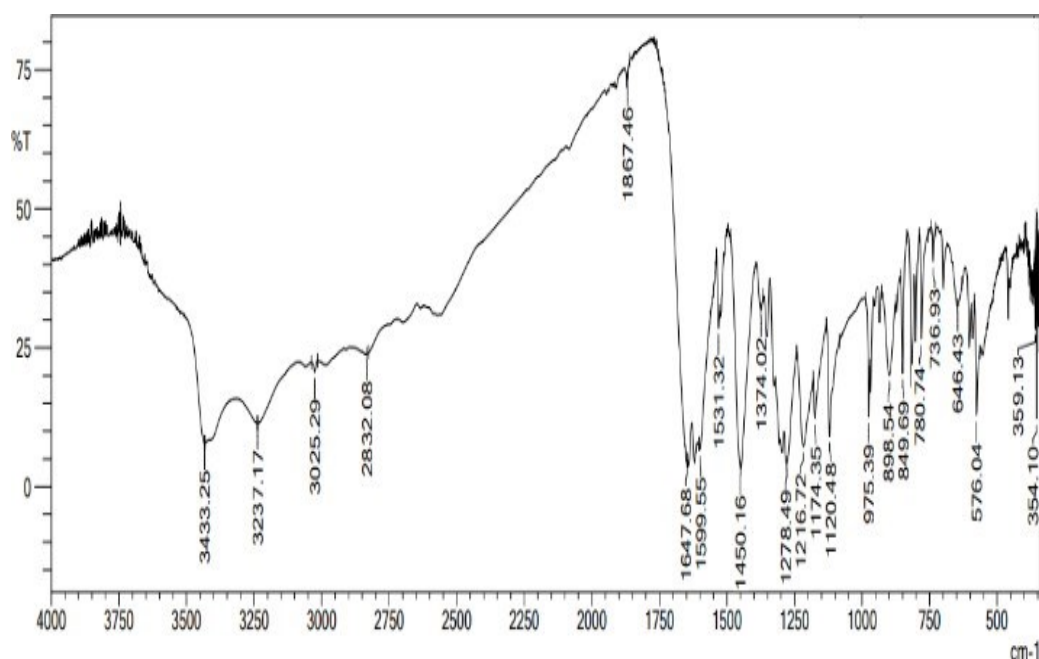


Fig 1. FTIR Spectrum show Physical Mixture

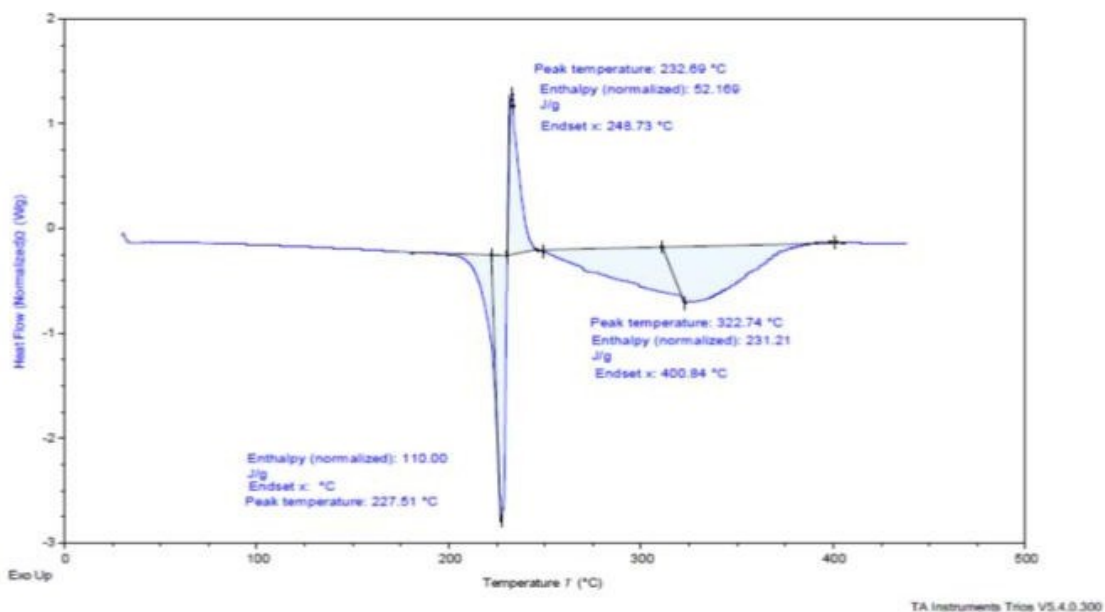
Wavenumber (cm ⁻¹)	Assignment	Interpretation
3433.25	O–H stretching / N–H stretching	Broad band indicating hydrogen-bonded hydroxyl groups from caffeic acid and amine groups of chitosan , suggesting strong intermolecular interaction

3237.17	N–H stretching (amide/amine)	Confirms presence of chitosan primary amine groups
3052.29	Aromatic C–H stretching	Characteristic of phenyl ring of caffeic acid
2832.08	Aliphatic C–H stretching	Associated with chitosan backbone
1647.68	Amide I (C=O stretching)	Chitosan amide group; possible interaction with caffeic acid carboxyl group
1599.55	N–H bending / aromatic C=C	Overlapping of chitosan amine bending and caffeic acid aromatic ring
1531.32	Amide II (N–H bending)	Confirms chitosan structure
1450.16	CH ₂ bending	Polysaccharide backbone of chitosan
1374.02	O–H bending	Phenolic hydroxyl groups of caffeic acid
1278.49	C–O stretching (phenolic)	Confirms presence of caffeic acid
1216.72, 1167.35	C–O–C stretching	Glycosidic linkages of chitosan
1120.48	C–O stretching	Polysaccharide skeleton
975.39	C–C stretching	Chitosan structure
889.54, 849.69	β-glycosidic linkages	Typical of chitosan
780.74, 736.93	Aromatic C–H bending	Caffeic acid aromatic ring
646.43, 576.04	Skeletal vibrations	Polymer matrix confirmation
359.13, 354.10	Low-frequency skeletal modes	Composite structure stabilization

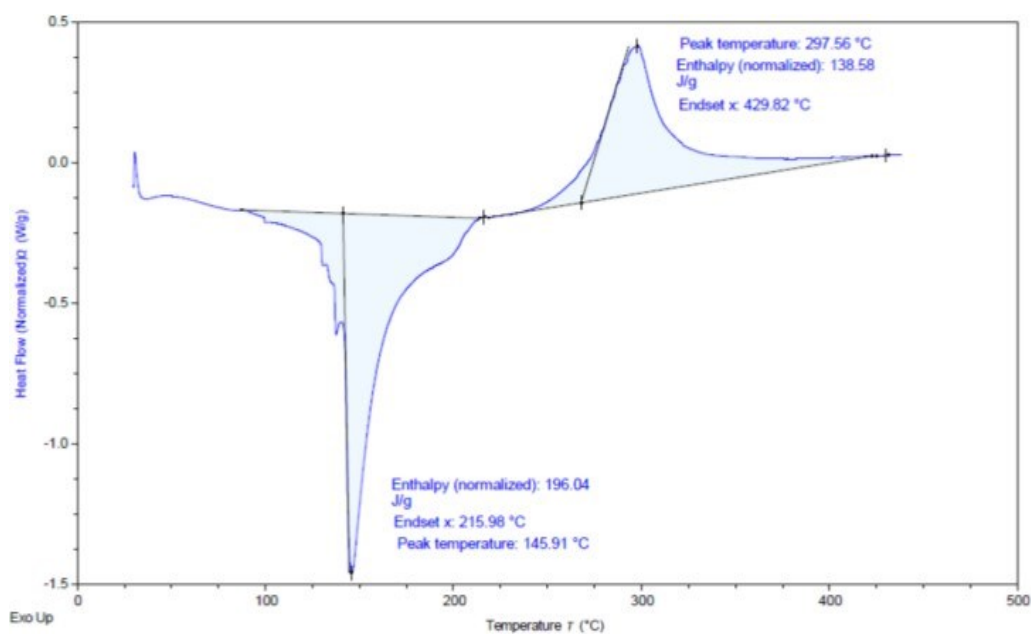
Table 3 : FTIR Interpretation Chart of physical mixture

7.1.2. Differential scanning calorimetry

The DSC thermogram of the physical Mixture of sample chitosan with caffeic acid exhibits a prominent endothermic peak at 145.91 °C with an enthalpy of 196.04 J/g and an endset at 215.98 °C, corresponding to the melting of a crystalline component, while a broad exothermic peak at 297.56 °C with an enthalpy of 138.58 J/g and an endset at 429.82 °C indicates thermal decomposition of the material. The shift in melting point and variation in enthalpy compared with the pure components suggest possible molecular interaction or complex formation between the drug and excipient. Overall, the thermogram confirms good compatibility and thermal stability of the formulation up to approximately 290 °C.



a) Pure Drug



b) Physical Mixture

Fig 2. DSC thermogram showing of the a) Pure drug & b) Physical Mixture

Formulation Code	Drug release (%)	Drying Time (min)	Velocity (mpa.s)
FFG 1	94.42	11	7662.2
FFG 2	92.62	7	5263.5

FFG 3	94.53	8	4753.4
FFG 4	91.1	6	4753.6
FFG 5	97.31	10	8726.1
FFG 6	95.61	7	9394.4
FFG 7	97.88	11	10286
FFG 8	98.34	9	10294

Table 4 : Drug Release, Drying time, tensile strength, and Velocity value for Film forming Gel Formulations.

7.2. Characterization and fitting of data to the model

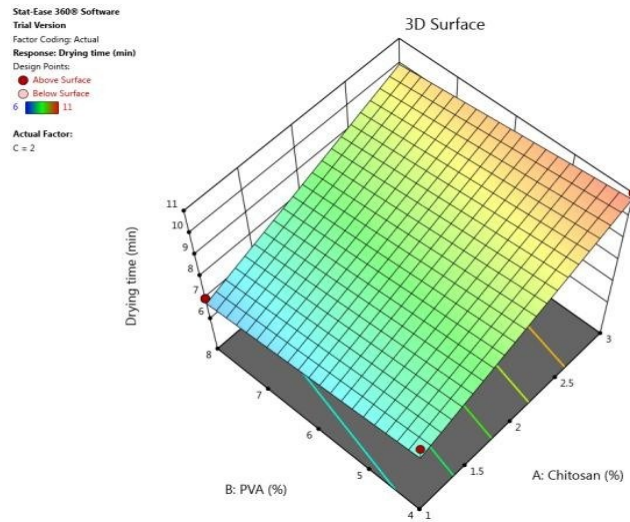
1. The three factor two level factorial design was employed to study the impact of formulation on tensile strength water evaporation value and drying time. St series of multiple experimental runs were generated for the application of response surface methodology and response thus obtained were unlisted in table 3.

2. These models are including first order second order quadratic models, were shifted to all response all three observed response were found to be match most accurately into the quadratic model based on the higher are value and minimal expected residual error sum of square (Prod>F value<0.0001). The highest standard error value for coefficient signifier that the nature of the relationship in quadric. ANOVA was performed to investigate the significant difference among the independent variable A,B, C.

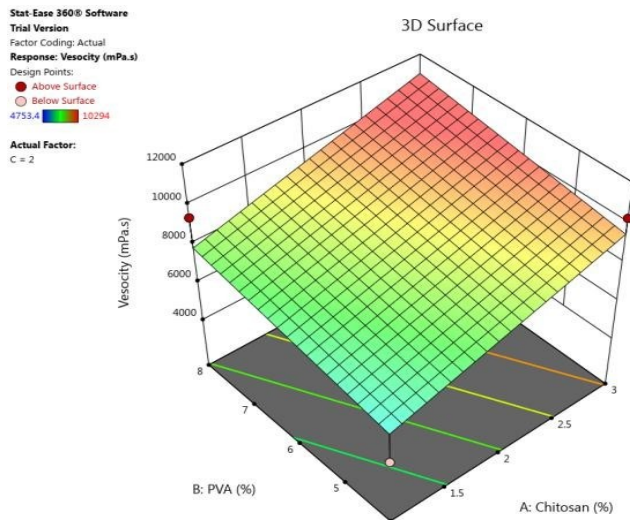
The significance of the model parameters was confirmed as the Prob > F values were found to be below 0.05. The

obtained F-values for the response variables Y1, Y2, and Y3 were 22.55, 8.52, and 12.49, respectively, suggesting that all the models were statistically significant. For Y1, the influential model terms included A, B, C, AB, AC, BC, A², B², and C². In the case of Y2, the significant factors were A, B, and C, whereas Y3 was notably affected by A, B, C, AB, AC, BC, A², B², and C².

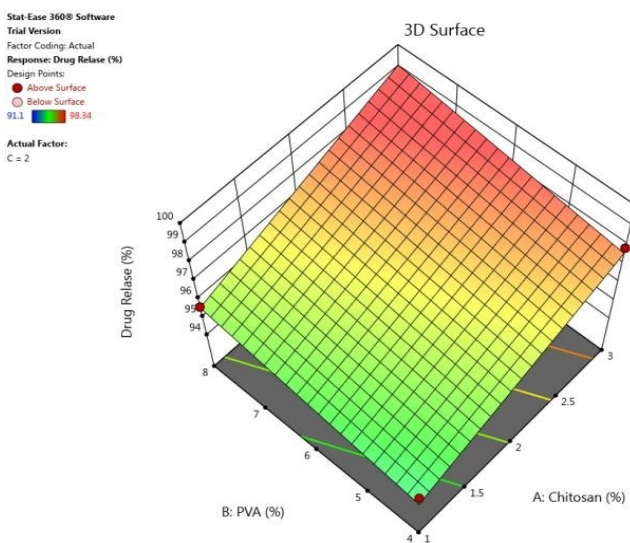
The correlation between the independent and dependent variables was described using polynomial equations, analyzed with specialized statistical software (Stat-Ease Inc., Minneapolis, USA). In these equations, positive coefficients denoted synergistic or enhancing effects that supported optimization, whereas negative coefficients represented adverse effects on the responses. The three-dimensional surface plots (Fig. 3) illustrate how variations in independent variables influence the dependent responses. The polynomial equations (Eq. 1, Eq. 2, and Eq. 3) along with the corresponding 3D plots for Y1, Y2, and Y3 are presented below.



(a)



(b)



(c)

Fig 3-dimension plots showing impact of independent variables on dependent variables (A) effect of chitosan and PA on drying time (B) effect of EC and PEG on water vapor evaporation value (C) effect of EC and DBS on tensile strength.

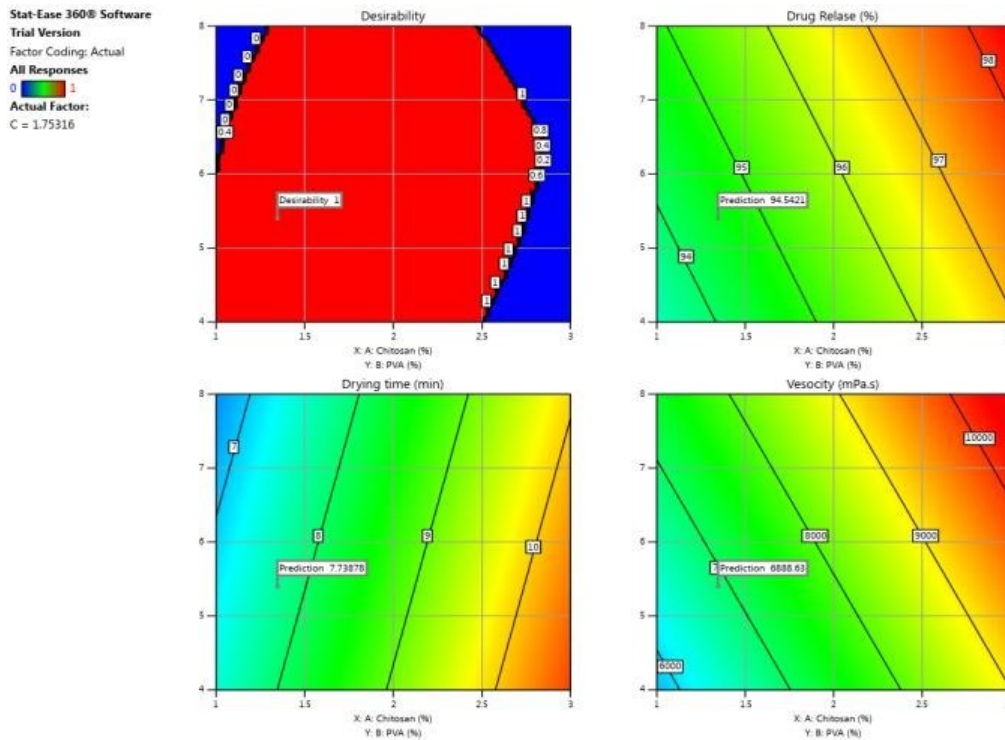


Fig 4 Contour Plots and Desirability Function for Optimization of Chitosan-Based Film Forming Gel Using 3² Factorial Design

For the response variable Y1, the positive coefficients of factors A and B in Equation (1) signify that the tensile strength increases with a higher concentration of ethyl cellulose. Conversely, the negative coefficient of factor C indicates that an increase in IPM concentration leads to a reduction in tensile strength. Regarding response Y2, water vapor absorption decreased as the concentrations of A and B increased, whereas a positive effect was observed with factor C. For response Y3, a decrease in drying time was noted with increasing concentrations of factors A and C, while an opposite trend was observed with factor B.

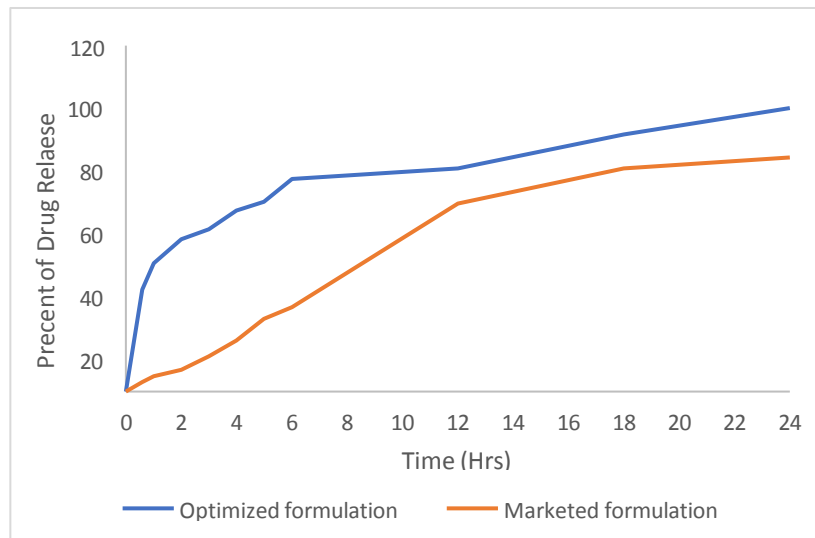


Fig. 5. Cumulative amount of drug release from Film forming Gel and Marketed Formulation

The formulation designated as FFG 8 was identified as the optimized composition, containing Chitosan, PVA and PEG at concentrations of 3% w/w, 8% w/w, and 2%

w/w, respectively. The optimized Film forming gel exhibited a Drug release of 98.34 ± 0.24 , a Drying time value of 9 min, and a Viscosity of 10294 mpa.s.

8. Evaluation of Physical Characteristics of the Film forming gel

The developed formulation appeared clear, uniform, and transparent, with no signs of external stickiness. Its viscosity was determined to be 10294 mpa.s, which was considered optimal for topical application as it allowed the formulation to spread easily and adhere well to the skin surface. The measured pH value was 5.8 ± 0.5 , which lies within the slightly acidic to neutral range, indicating that the formulation is skin-compatible and unlikely to cause irritation.

8.1. In-vitro Drug Release Studies

The in vitro release profile demonstrated that the test formulation exhibited a higher drug release rate compared to the marketed product. Initially, the drug-loaded film forming gel showed a rapid release phase, followed by a sustained release over the remaining duration of the study (Fig. 4).

The percentage cumulative drug release (% CDR) was calculated using the following formula:

$$\% \text{ Cumulative drug release (CDR)} = \frac{\text{Amt of the drug in the sample}}{\text{Amt of the drug in the donor compartment}} \times 100$$

After 6 hours of testing, the film forming gel formulation released 73.82 % of the drug, whereas the marketed formulation released 29.32 %. These findings indicate that the prepared film forming gel achieved significantly enhanced drug release compared to the marketed reference product (White and Turner, 2019).

9. Discussion

The present study focused on the development and optimization of a film-forming Gel formulation incorporating Caffeic acid as the active therapeutic agent. The formulation aimed to combine the advantages of a Gel application system with the protective and healing benefits of a thin, flexible film. The prepared formulation exhibited desirable physical and mechanical properties, indicating successful optimization of the polymeric matrix.

Chitosan, polyvinyl alcohol (PVA), and PEG were selected as key formulation components due to their ability to form an elastic, adhesive, and breathable film on the skin. The positive coefficients of ethyl cellulose and DBS in the model suggested their direct influence on improving tensile strength, as higher polymer and plasticizer concentrations enhanced film integrity and flexibility. Conversely, the negative coefficient of IPM indicated that excessive concentrations reduced tensile

strength, likely due to the increased film softness and plasticizing effect.

The viscosity of the optimized formulation (10294 mPa.s) was found to be ideal for topical application, ensuring smooth spreadability and adequate film formation without surface stickiness. The pH value (5.8 ± 0.5) was within the physiological range of the skin, confirming its compatibility and non-irritating nature. These characteristics collectively demonstrated the formulation's suitability as a topical wound dressing system.

The in vitro drug release profile revealed a biphasic pattern—an initial burst release followed by a sustained release phase. This release behavior is advantageous for wound management, as it ensures rapid initial drug availability to reduce microbial load, followed by prolonged release for continued therapeutic effect. The cumulative drug release from the optimized formulation (73.82% after 6 hours) was significantly higher than that of the (Fig 5) marketed formulation (29.32%), indicating better diffusion characteristics and controlled drug delivery from the polymeric film matrix.

Overall, the optimized Film forming gel formulation exhibited excellent physical characteristics, stable pH, appropriate viscosity, and favorable drug release kinetics. These results suggest that the developed film-forming system can serve as a promising alternative to traditional wound dressings by offering improved adhesion, controlled drug delivery, and enhanced patient comfort

10. Conclusion

In this study, a film-forming gel was successfully developed, optimized, and evaluated. Film forming gel represent an advanced approach for topical application on injured skin, as they not only form a protective and moist environment conducive to healing but also facilitate localized drug delivery Caffeic Acid, known for its antioxidant activity, served as the active agent of choice for promoting effective wound therapy. The overall findings indicate that the formulated caffeic acid based film forming gel exhibits strong potential as an effective wound-healing system and may serve as a promising alternative to conventional wound dressings.

Acknowledgment

The authors express their sincere gratitude to the management of Teerthanker Mahaveer University, Moradabad, Uttar Pradesh, for providing the necessary

facilities and academic environment to carry out this research work.

The authors also extend heartfelt thanks to the faculty members and staff of the Department of Pharmaceutical Sciences for their valuable guidance, encouragement, and continuous support throughout the research work.

We are grateful to all colleagues and research scholars who contributed directly or indirectly to the completion of this work..

REFERENCE

- Pereira, R., Mendes, A., & Oliveira, M. B. (2018). Film-forming systems for topical drug delivery. *European Journal of Pharmaceutics and Biopharmaceutics*, 132, 1–14. <https://doi.org/10.1016/j.ejpb.2018.08.012>
- Felton, L. A. (2013). Film coating of oral solid dosage forms. *AAPS PharmSciTech*, 14(2), 511–524. <https://doi.org/10.1208/s12249-013-9939-1>
- Montgomery, D. C. (2017). *Design and analysis of experiments* (9th ed.). Wiley.
- Beg, S., Hasnain, M. S., Rahman, M., & Swain, S. (2019). Application of Quality by Design (QbD)-based DoE in pharmaceutical formulation development. *Drug Development and Industrial Pharmacy*, 45(10), 1565–1584. <https://doi.org/10.1080/03639045.2019.1645789>
- Abd El-Kader, M.F.H., Ahmed, M.K., Elabbasy, M.T., Afifi, M., Menazea, A.A., 2021. Morphological, mechanical and biological properties of hydroxyapatite layers deposited by pulsed laser deposition on alumina substrates. *Surf. Coat. Technol.* 409, 126861 <https://doi.org/10.1016/j.surfcoat.2021.126861>.
- Aggarwal, S., Thakur, A., Sharm, A., 2022. Development and evaluation of ketoprofen loaded floating microspheres for sustained delivery. *Mater. Today: Proc.* 68, 647–652.
- Aldabahi, A., Ahmed, M.K., Govindasami, P., Rahaman, M., Anter, A., 2020. Core-shell Au@Se nanoparticles embedded in cellulose acetate/polyvinylidene fluoride scaffold for wound healing. *J. Mater. Res. Technol.* 9, 15045–15056. <https://doi.org/10.1016/j.jmrt.2020.10.079>.
- Anter, A., Ismail, A.M., Samy, A., 2021. Novel green synthesis of zinc oxide nanoparticles using orange waste and its thermal and antibacterial activity. *J. Inorg. Organomet. Polym Mater.* 31, 1–10. <https://doi.org/10.1007/s10904-021-02074-2>.
- Atiyeh, B.S., Costagliola, M., Hayek, S.H., Dibo, S.A., 2007. Effect of silver on burn wound infection control and healing: a review of the literature. *Burns* 33, 139–148.
- Aziz, Z., Abu, S.F., Chong, N.J., 2012. A systematic review of silver-containing dressings and topical silver agents (used with dressings) for burn wounds. *Burns* 38 (3), 307–318. <https://doi.org/10.1016/j.burns.2011.09.020>.
- Barchitta, M., Maugeri, A., Favara, G., Lio, R.M.S., Evola, G., Agodi, A., Basile, G., 2019. Nutrition and wound healing: an overview focusing on the beneficial effects of curcumin. *Int. J. Mol. Sci.* 20, 1119.
- Brown, S.M., Davis, E.R., 2019. Statistical optimization of liquid bandage formulation for wound care. *Pharm. Formulation Sci.* 8 (2), 56–71.
- Cañedo-Dorantes, L., Cañedo-Ayala, M., 2019. Skin acute wound healing: a comprehensive review. *Int. J. Inflamm.* 2019, 3706315.
- El Ashram, S., El-Samad, L.M., Basha, A.A., El Wakil, A., 2021. Naturally-derived targeted therapy for wound healing: beyond classical strategies. *Pharmacol. Res.* 170, 105749.
- El-Newehy, M., Anter, A., Thamer, B., Elnaggar, M., 2021. Preparation of antibacterial film-based biopolymer embedded with vanadium oxide nanoparticles using one-pot laser ablation. *J. Mol. Struct.* 1225, 129163.
- Eming, S.A., Martin, P., Tomic-Canic, M., 2014. Wound repair and regeneration: mechanisms, signaling, and translation. *Sci. Transl. Med.* 6, 265.
- Fathi, A., Ahmed, M., Afifi, M., Anter, A., Uskokovic, V., 2020. Taking hydroxyapatite-coated titanium implants two steps forward: surface modification using graphene mesolayers and a hydroxyapatite-reinforced polymeric Scaffold. *ACS Biomater Sci. Eng.* 7 <https://doi.org/10.1021/acsbiomaterials.0c01105>.
- Jodar, K.P.S., Balc, V.M., Chaud, V.M., Tubino, M., Yoshida, V.M.H., Oliveira, M.J., et al., 2015. Development and characterization of a hydrogel containing silver sulfadiazine for antimicrobial topical applications. *J. Pharm. Sci.* 104, 2241–2251.
- Monavarian, M., Kader, S., Moeinzadeh, S., Jabbari, E., 2019. Regenerative scar-free skin wound healing. *Tissue Eng. Part B Rev.* 25, 294–311.
- Morsi, N.M., Abdelbary, G.A., Ahmed, M.A., 2014. Silver sulfadiazine based cubosome hydrogels for topical treatment of burns: development and in vitro/in vivo characterization. *Eur. J. Pharm. Sci.* 86, 178–189.
- Pereira, G.G., Guterres, S.S., Balducci, A.G., Colombo, P., Sonvico, F., 2014. Polymeric films loaded

- with vitamin E and Aloe vera for topical application in the treatment of burn wounds. *Biomed. Res. Int.* 2014, 1–9.
22. Raja, S.K., Garcia, M.S., Isseroff, R.R., 2007. Wound re-epithelialization: modulating keratinocyte migration in wound healing. *Front. Biosci. (landmark Ed)* 12, 2849–2868.
23. Ranade, S., Bajaj, A., Londhe, V., Kao, D., Babul, N., 2014. Fabrication of polymeric film forming topical gels. *Int. J. Pharm. Sci. Rev. Res.* 26 (2), 306–313.
24. Robson, M.C., Steed, D.L., Franz, M.G., 2001. Wound healing: biologic features and approaches to maximize healing trajectories. *Curr. Probl. Surg.* 38, 72–140.
25. Rodeheaver, G.T., Pettry, D., 1976. Silver sulfadiazine: in vitro antibacterial activity. *Antimicrob Agents Chemother.* 10 (5), 768–772. <https://doi.org/10.1128/aac.10.5.768>.
26. Sharma, A., Harikumar, S.L., 2020. Quality by design approach for development and optimization of nitrendipine-loaded niosomal gel for accentuated transdermal delivery. *Int. J. Appl. Pharm.* 12 (5), 181–189. <https://doi.org/10.22159/ijap.2020v12i5.38639>.
27. Sharma, A., Singh, A.P., Harikumar, S.L., 2020. Development and optimization of nanoemulsion based gel for enhanced transdermal delivery of nitrendipine using box-behnken statistical design. *Drug Dev. Ind. Pharm.* 46 (2), 329–342. <https://doi.org/10.1080/03639045.2020.1721527>.
28. Sharma, A., Thakur, R., Sharma, R., 2022. Development and optimization of candesartan cilexetil nasal gel for accentuated intranasal delivery using central composite design. *Mater. Today: Proc.* <https://doi.org/10.1016/j.matpr.2022.11.221>.
29. Singh, B., Sharma, S., Dhiman, A., 2013. Design of antibiotic-containing hydrogel wound dressings: biomedical properties and histological study of wound healing. *Int. J. Pharm.* 457, 82–91.
30. Smith, J.D., Johnson, A.R., 2020. Advanced wound care using silver sulfadiazine-loaded liquid bandages. *J. Wound Healing Res.* 10 (3), 123–137.
31. Süntar, I., Küpeli Akkol, E., Keles, H., Yesilada, E., Sarker, S.D., 2013. Exploration of the wound healing potential of *Helichrysum graveolens* (Bieb.) Sweet: isolation of apigenin as an active component. *J. Ethnopharmacol.* 149 (1), 103–110. <https://doi.org/10.1016/j.jep.2013.06.006>.
32. Suresh, C., Abhishek, S., 2016. pH sensitive in situ ocular gel: a review. *J. Pharma Sci. Bioscienti Res.* 6 (5), 684–694.
33. Tas, C., Ozkan, Y., Savaser, A., Baykara, T., 2003. In vitro release studies of chlorpheniramine maleate from gels prepared by different cellulose derivatives. *II Farmaco.* 58, 605–611.
34. Thakur, R., Sharma, A., 2019. An overview of mucoadhesive thermoreversible nasal gel. *Asian J. Pharm. Res. Dev.* 9 (4), 158–168. <https://doi.org/10.22270/ajprd.v9i4.994>.
35. Thampy, R., 2022. Development, optimization and evaluation of silver sulphadiazine loaded nano fibrous scaffold as wound healing. *Int. J. Drug Develop. Res.* 14 (10), 978.
36. Tort, S., Demiröz, F.T., Cevher, S.C., Sarıbas, S., Özoğul, C., Acartürk, F., 2020. The effect of a new wound dressing on wound healing: biochemical and histopathological evaluation. *Burns* 46, 143–155.
37. Tottoli, E.M., Dorati, R., Genta, I., Chiesa, E., Pisani, S., Conti, B., 2020. Skin wound healing process and new emerging technologies for skin wound care and regeneration. *Pharmaceutics.* 12, 735.
38. Venkataraman, M., Nagarsenker, M., 2013. Silver sulfadiazine nanosystems for burn therapy. *AAPS Pharm. Sci. Tech.* 14 (1), 215–223.
39. Vij, N.N., Saudagar, R.B., 2014. Formulation, development, and evaluation of film forming gel for prolonged dermal delivery of terbinafine hydrochloride. *Indian J. Pharm. Sci. Res.* 5 (9), 537–554.
40. Walendziak, W.P., Kozłowska, J., 2021. Design of sodium alginate/gelatin-based emulsion film fused with polylactide microparticles charged with plant extract. *Materials* 14, 745. <https://doi.org/10.3390/ma14040745>.
41. Wallace, H.A., Basehore, B.M., Zito, P.M., 2017. *Wound Healing Phases*; StatPearls Publishing: Treasure Island, FL, USA.